Editors' Suggestion

Turbulence modulation by suspended finite-sized particles: Toward physics-based multiphase subgrid modeling

S. Balachandar [*]
University of Florida, Gainesville, Florida, 32608, USA

C. Peng [†]
Shandong University, Jinan, Shandong, China

L.-P. Wang [‡]
Southern University of Science and Technology, Shenzhen, Guangdong, China

(Received 22 October 2023; accepted 1 March 2024; published 11 April 2024)

The presence of a dispersed phase substantially modifies small-scale turbulence. However, there has not been a comprehensive mechanistically based understanding to predict turbulence modulation. Based on the energy flux balance, we propose a theoretical model to predict the turbulent kinetic energy modulation in isotropic turbulence due to the dispersed phase. The comparison between model predictions and results from prior particle-resolved simulations and existing high-fidelity experiments supports the performance of the model over a range of turbulence and particle parameters. The model is then used to explore turbulence modulation characteristics over a wider parameter space formed by five independent system-controlling parameters, showing rather complicated dependence on the particle size and particle-to-fluid density ratio.

DOI: 10.1103/PhysRevFluids.9.044304

I. INTRODUCTION

The presence of particles, droplets, or bubbles in a flow substantially alters the nature of multiphase turbulence, rendering the problem far more complex than single-phase turbulence. In the two-way coupled regime, the continuous phase influences the dynamics and the spatial distribution of the suspended dispersed phase, while the suspended particulates (henceforth refers to particles, droplets, and bubbles) modulate the character of turbulence in the continuous phase. In homogeneous isotropic turbulence laden with particles of negligible sedimentation, a pivot scale of the order of the particle diameter (D) is found to distinguish whether turbulence is attenuated or augmented [1–6]. This pivot scale depends not only on the particle size, but also on the ratio of particle size to the Taylor microscale and particle-to-fluid density ratio [4]. In inhomogeneous and wall-bounded flows with sedimenting particles, turbulence modulation is more complex. In some cases, the entire turbulence is due to the suspended particles, without a pivot scale [7,8].

Several criteria for turbulence modulation have been advanced in the past. Gore and Crowe [9] suggested that turbulence is augmented if the ratio of D to the characteristic size of the energy-containing eddies is greater than 0.1, and otherwise suppressed. On the other hand, Elghobashi and Truesdell [10] observed turbulence enhancement even for particles of diameter comparable to the

[*]bala1s@ufl.edu
[†]pengcheng@sdu.edu.cn
[‡]wanglp@sustech.edu.cn

Kolmogorov scale (η). The Gore and Crowe criterion was recently updated by Oka and Goto [5] by requiring D to be not only below the integral length scale but also larger than the Taylor microscale divided by the square root of particle-to-fluid density ratio for turbulence attenuation. Hetsroni [11] recommended particle Reynolds number $Re_p > 400$ as the criterion for turbulence enhancement resulting from vortex shedding. Bagchi and Balachandar [12], however, observed vortex shedding to initiate at much lower Re_p in the presence of free-stream turbulence. Tanaka and Eaton [13] introduced a particle momentum number as the nondimensional parameter to distinguish between turbulence augmentation and attenuation. A similar criterion has also been introduced by Luo, Luo, and Fan [14]. Peng *et al.* [6] presented empirical correlations that well predict multiphase turbulence modulation in the absence of gravitational effects.

The purpose of this work is to develop a physics-based closure model for subgrid turbulence that can be used in multiphase large eddy simulations (LES). We focus on the homogeneous isotropic flow configuration, but desire the closure model to be universal with applicability for a wide range of particle sizes (including $D \gg \eta$), volume, and mass fractions. Furthermore, we want the model to account for the inertial and gravitational effects on the particles as well as the dissipative effect of interparticle collisions at higher volume fractions.

The limited scope of the present work on turbulence modulation compared to the broader quest of earlier efforts by others must be emphasized. The mesoscale state of the dispersed multiphase flow is considered to be known, e.g., as in LES, and we limit the quest to modeling of turbulence modulation at the micro or subgrid scales. Such an understanding of turbulence modulation along with well-developed closure models of single-phase turbulence may provide robust and general multiphase subgrid closures. The modeling of subgrid turbulence, however, remains formidable as a very wide range of scales and a large number of particles are involved. Thus, turbulence modulation and its modeling remain formidable even when limited to subgrid scales.

Conceptually, we distinguish two different mechanisms of turbulence modulation. At the microscale, the slip velocity between the particles and the fluid due to particle inertia, finite size, and gravity results in pseudoturbulence, altering the spectral distribution of kinetic energy. At the mesoscale, turbulence may be modulated by the gravitational influence on a nonuniform distribution of particulates. Buoyancy-induced instabilities enhance turbulence, while stable stratification can strongly suppress turbulence [15,16]. By limiting attention to only turbulence modulation at the subgrid scale, we avoid the influence of mesoscale turbulence modulation. Furthermore, we shall assume the particulate phase to be uniformly distributed in the theoretical analysis. We present a physics-based model to predict turbulence modulation and test it against particle-resolved (PR) simulation and experimental results for isotropic turbulence [1,3,5,6,17–21] and the central region of turbulent channel flow [22,23] that are available in the literature. The model is then used to illustrate turbulence modulation over a wider parameter space.

We envision the model to be used in the following way. In an LES, given the resolved scale fluid and particle properties at each grid cell, unresolved subgrid turbulence can be estimated using approaches well developed in single-phase turbulence and the present model can then be used to calculate turbulence modulation due to suspended dispersed phase. This approach remains applicable even in the case of Reynolds averaged Navier Stokes (RANS) simulation, where only the mean flow is resolved. In this case, at each grid cell, given the mean fluid and particulate properties, a standard single-phase RANS closure model can be used to first estimate the level of local single-phase turbulent fluctuation, which can then be corrected with the present model to obtain the corresponding multiphase closure.

The rest of the paper is organized as follows. First, in Sec. II, we present the theoretical model of turbulence modulation. The accuracy of the theoretical model is evaluated in Sec. III, by comparing the model prediction against available experimental and PR simulation results. The available experimental and PR simulation results cover only a range of the five-parameter space. So, in Sec. IV, we vary the parameter values over a very wide range and use the theoretical model to explore the effect on turbulence modulation. Finally, in Sec. V, key conclusions are presented with recommendations for future studies.

II. THEORETICAL MODEL

Consider a Euler-Euler (EE) LES of particle-laden flow with a random distribution of particles in a finite-volume cell of size $\Delta x \gg D, \eta$. Let the mean fluid velocity $\mathbf{u}$, particle velocity $\mathbf{v}$, and particle volume fraction ϕ be known within the cell. These are cell-averaged mean quantities obtained by averaging over the subgrid fluid and particle velocity variations (here we have ignored the usual overbar notation used to denote the filtered variables in LES). From the energy transfer of the resolved-scale turbulence, we estimate the flux of kinetic energy to the subgrid scales and denote it ϵ. In the case of single-phase turbulence, following standard turbulence argument, we can take the flux of subgrid kinetic energy to be equal to the average viscous dissipation rate within the fluid that occupies the cell. In the multiphase turbulence we take ϵ to be the energy flux to the subgrid volume., the multiphase LES subgrid modeling quest is to predict closure quantities such as (i) the subgrid fluid Reynolds stress, (ii) particle Reynolds stress, and (iii) mean and rms force acting on the particles [24]. Here, the focus will be on quantifying turbulence modulation in terms of the ratio between multi and single-phase subgrid fluid Reynolds stress.

In the isotropic limit, the four key controlling parameters are [6] (i) D/η, (ii) subgrid turbulence intensity measured in terms $Re_\Delta = \epsilon^{1/3}(\Delta x)^{4/3}/\nu$, (iii) particle-to-fluid density ratio $\rho = \rho_p/\rho_f$, and (iv) the local particle volume fraction ϕ. In the presence of a mean relative velocity (i.e., when $\mathbf{u} \neq \mathbf{v}$), subgrid Reynolds stress tensor ceases to be isotropic—it is only axisymmetric. There is an additional parameter: (v) relative mean slip velocity between the fluid and particulate phases, $u_r = |\mathbf{u} - \mathbf{v}|/u_k$, where the denominator is the Kolmogorov velocity. We propose the following energy flux balance within the subgrid [5,17,25]:

$$\epsilon + N\, 3\pi \nu D\, \Phi |\mathbf{u} - \mathbf{v}|^2 = C_{c,mp} \frac{k_{f,mp}^{3/2}}{\Delta x} + C_p N\, 3\pi \nu D\, \Phi'\, \Delta u^2 + C_{co} \frac{\rho \phi^2}{D} \Delta u\, k_p, \tag{1}$$

where the second term on the left-hand side is the rate of work input on the subgrid fluid-particle system due to mean relative motion of all the $N = \phi/(\pi D^3/6)$ particles. This term contributes to the subgrid energy transfer in addition to that from cascading turbulence represented by ϵ. $\Phi(Re, \phi)$ represents correction to Stokes drag due to the finite value of $Re = |\mathbf{u} - \mathbf{v}|D/\nu$ and volume fraction ϕ (see [26–28]). This term, along with two additional contributions arising from particle acceleration and interparticle collision, was rigorously derived in [17,25]. As shown by them, the other two contributions are generally small and therefore not included in the above balance.

The first term on the right-hand side represents fluid phase dissipation in the bulk, where $k_{f,mp}$ is the subgrid fluid kinetic energy in the multiphase system. From dimensional arguments, dissipation is taken to be the cube of the velocity scale divided by the length scale Δx of the subgrid. The second term is dissipation in the immediate neighborhood of the particles that do not contribute to the bulk fluid turbulence. The local dissipation depends on the fluctuating relative velocity Δu between the particle and the surrounding fluid, which again can be taken to depend on the parameters listed above. In this term, Φ' is a correction to Stokes drag based on $Re' = \Delta u D/\nu = (\Delta u/u_k)(D/\eta)$. From the proportionality $\Phi'(Re', \phi) \propto C_D Re'$ (C_D is the drag coefficient), we obtain the scaling $\Phi'(Re', \phi) \propto \Delta u$. Substituting this into the second term on the right hand side, we can see that this term is $\propto \Delta u^3$. This cubic scaling is in agreement with the closure model presented in [5].

The third term accounts for the dissipative effect of interparticle collisions. Each inelastic collision results in the post-collision energy of the particles being lower than their precollision state. The energy lost by interparticle collisions in turn comes from the kinetic energy of the fluid. A derivation of this term is provided in the Appendix and in this term, k_p is subgrid particle kinetic energy. This term is expected to play a role only at higher volume fractions when interparticle collisions are frequent so that the dissipative effect of inelastic collisions contributes to overall energy balance. Classification of multiphase flows into one-way, two-way, and four-way coupled regimes [10,29,30] suggest that when local volume fraction $\phi \gtrapprox 10\%$ the flow can be considered to be four-way coupled with interparticle collisional effect becoming important. The empirical coefficients $C_{c,mp}$, C_p, and C_{co} can not be determined by the scaling arguments employed in expressing the different contributions. Here, they will be determined by fitting the available experimental and PR simulation data.

Given ϵ, we calculate Kolmogorov length, time, and velocity scales as $\eta = \nu^{3/4}/\epsilon^{1/4}$, $\tau_k = \eta^{2/3}/\epsilon^{1/3}$, and $u_k = (\epsilon\eta)^{1/3}$. The scaling relation for slip velocity by Balachandar [31,32] can be restated as

$$\frac{\Delta u}{u_k} = \begin{cases} |1-\beta| St_k & \text{(i) if } \tau_p < \tau_k \\ |1-\beta| St_k^{1/2} & \text{(ii) if } \tau_k < \tau_p < \tau_\Delta \\ |1-\beta| Re_\Delta^{1/4} & \text{(iii) if } \tau_p > \tau_\Delta \\ u_r & \text{(iv) if } u_r \text{ dominates,} \end{cases} \tag{2}$$

where $\beta = 3/(2\rho+1)$ is the density parameter and it ranges from $\beta = 0$ for heavy particles to $\beta = 3$ for lighter bubbles. The particle time scale is $\tau_p = (2\rho+1)D^2/(36\nu\Phi')$, $St_k = \tau_p/\tau_k$ is the particle Stokes number based on the Kolmogorov time scale, and $\tau_\Delta = (\Delta x)^{2/3}/\epsilon^{1/3}$. As can be seen from the equation, the estimate of relative velocity depends on the particle size regime. The four regimes are as follows: (i) small particles whose time scale is smaller than the Kolmogorov time scale. These particles respond well to all the subgrid scales; (ii) medium-sized particles whose time scale is larger than the Kolmogorov time scale but smaller than the time scale of the largest subgrid eddies. These medium sized particles respond well to the larger subgrid eddies but not to the smaller subgrid eddies; (iii) large particles whose time scale exceeds the time scale of the largest unresolved subgrid eddies; and (iv) scenarios where mean relative velocity dominates. In the first three regimes, Δu is dictated by the inertial response of the particles to unresolved subgrid turbulent eddies, whereas in regime four the relative velocity is dominated by the difference in mean motion. We note that $\tau_p/\tau_k = (2\rho+1)(D/\eta)^2/(36\Phi')$ and $\tau_p/\tau_\Delta = (\tau_p/\tau_k)/\sqrt{Re_\Delta}$. A simplified evaluation of the implicit equation, Eq. (2), is discussed in [31]. Equation (2) was obtained in the absence of two-way coupling. With the effect of turbulence modulation, the estimated slip velocity must be adjusted. A simple correction will be to multiply the right hand side of Eq. (2) by $\sqrt{k_{f,mp}/k_{f,sp}}$. Note that the simple model, Eq. (2), offers a continuous variation of Δu with τ_p.

In order to evaluate turbulence modulation as the ratio, $k_{f,mp}/k_{f,sp}$, between multi and single-phase kinetic energy, for the same energy flux ϵ, we first define the single-phase limit as

$$\epsilon = C_{c,sp} k_{f,sp}^{3/2}/\Delta x, \tag{3}$$

which is similar to the first term on the right-hand sides of Eq. (1). We divide Eq. (1) by the above single-phase ϵ to obtain

$$\left(C' + C_{co}\rho\phi^2 Re_\Delta^{1/2} \frac{\Delta u}{u_{k,sp}} \frac{k_p}{k_{f,mp}} \frac{\eta_{sp}}{D}\right)\left(\frac{k_{f,mp}}{k_{f,sp}}\right)^{3/2} + 18 C_p\phi\, \Phi' \left(\frac{\Delta u}{u_{k,sp}} \frac{\eta_{sp}}{D}\right)^2 \frac{k_{f,mp}}{k_{f,sp}}$$
$$= 1 + 18\phi\, \Phi\, u_r^2 \left(\frac{\eta_{sp}}{D}\right)^2, \tag{4}$$

where $C' = C_{c,mp}/C_{c,sp}$. We recognize the possibility that the single-phase coefficient $C_{c,sp}$ can be different from that of the multiphase limit. This introduces C' as an empirical coefficient that must be determined. The above is an implicit equation for the ratio $k_{f,mp}/k_{f,sp}$ in terms of the five input parameters (note $\Delta u/u_{k,sp}$ is a function of the five parameters).

In the limit of significant dissipation due to interparticle collisions, particle-to-fluid subgrid kinetic energy ratio, $k_p/k_{f,mp}$, must also be specified. This ratio corresponds to particle kinetic energy compared to the local fluid kinetic energy. In the limit of zero mean slip velocity (i.e., $u_r \to 0$), both fluid and particle velocity fluctuations can be considered isotropic and the ratio of their kinetic energy is given by the classic result [33]

$$\frac{k_p}{k_{f,mp}} = \frac{1}{(1+St)}, \tag{5}$$

where the Stokes number St is the ratio of particle time scale to Lagrangian fluid integral time scale seen by the particle. The expression is a rigorous result if the Lagrangian fluid velocity correlation seen by the particle is of the exponential form. The above expression simply reflects the fact that velocity fluctuations of inertial particles of large St is smaller than those of the surrounding fluid. In the case of nonzero relative velocity, particle velocity fluctuation is anisotropic and the kinetic energy ratio along the longitudinal and transverse directions are different, whose estimated values were obtained by Wang and Stock [34].

III. EVALUATION OF THEORY

We now evaluate the model by reproducing results on turbulence modulation from past PR simulations and experiments. In obtaining Eq. (4) it has been taken that the energy flux ϵ into the subgrid scales is the same for both single and multiphase cases. This is an appropriate condition for LES closure, since the state of the local resolved scales dictate the rate of energy flux to the subgrid scale. However, in the forced isotropic simulations to be compared, the forcing at the largest scales is typically maintained the same between the single and multiphase simulations. This constant forcing does not guarantee the dissipation rates of single and multiphase turbulence to be the same, since the energy input depends on the inner product between the forcing and the fluid velocity. Fortunately, the dissipation rates of single and multiphase turbulence are independently reported in these simulations. This difference in single vs multiphase dissipation is accounted for in the theory with the following modification. In the left-hand sides of Eqs. (3) and (1), the energy flux is differentiated as ϵ_{sp} and ϵ_{mp}. With this modification, we obtain

$$C'\left(\frac{k_{f,mp}}{k_{f,sp}}\right)^{3/2} + 18C_p\phi\,\Phi'\left(\frac{\Delta u}{u_{k,sp}}\,\frac{\eta_{sp}}{D}\right)^2\frac{k_{f,mp}}{k_{f,sp}} = \frac{\epsilon_{mp}}{\epsilon_{sp}} + 18\phi\,\Phi\,u_r^2\left(\frac{\eta_{sp}}{D}\right)^2. \tag{6}$$

In the above equation we have ignored the effect of interparticle collisions because we will be evaluating the theoretical prediction against simulations and experiments performed at sufficiently low particle volume fractions, where interparticle collisions are rare and do not contribute. Given the five nondimensional parameters, which characterize the multiphase flow, namely D/η, Re_λ, ρ, ϕ, and u_r, the above equation can be solved for the ratio $k_{f,mp}/k_{f,sp}$, with the additional information on the dissipation ratio $\epsilon_{mp}/\epsilon_{sp}$. The solution procedure is not explicit due to the fact that both the above equation as well as the one for slip velocity are implicit. In the application of the present model in an LES, Re_Δ will be calculated based on the grid size and it is representative of the Reynolds number of subgrid turbulence, whose modulation is of interest. However, when evaluating the model against existing PR simulations, we must choose a Reynolds number that appropriately characterizes the particle-resolved turbulence. Given the Taylor microscale Reynolds number, we evaluate Re_Δ from the relation $Re_\Delta = Re_\lambda^2/15$, where we have used the definition $Re_\lambda = \sqrt{15}(u')^2/\sqrt{\epsilon\nu}$.

We consider 60 PR simulations and four experiments from eight different sources. They cover $D/\eta \in [0.96, 17.77]$, $Re_\lambda \in [32.95, 240]$, $\rho \in [0, 2080]$, and $\phi \in [7.17 \times 10^{-6}, 0.12]$. Particle settling is negligible and therefore, $u_r = 0$. We observe good agreement for $C_p = 1.0$ and

$$C' - 1 = \min\{(\rho - 1)\phi, 0.48\}\{1 - \sigma[\ln(St_k) - \ln(500))]\}, \tag{7}$$

where σ is the sigmoid function. Figure 1 presents the actual measured value of turbulence modulation $(k_{f,mp}/k_{f,sp})_{DNS,exp}$ plotted again that is predicted by theory. We observe the agreement to be quite good and comparable in performance to the fits given in [5,6]. It should be noted that turbulence modulation presented in Fig. 1 is related to the nature of force used to maintain stationary turbulence. Except in the simulations of Oka and Goto [5], in all other cases considered, due to the nature of forcing, turbulence modulation is accompanied by a reduction in dissipation ratio. In all cases considered, with a different forcing methodology employed in the single-phase and multiphase turbulence cases, we expect different dissipation and kinetic energy ratios. However, the two will be

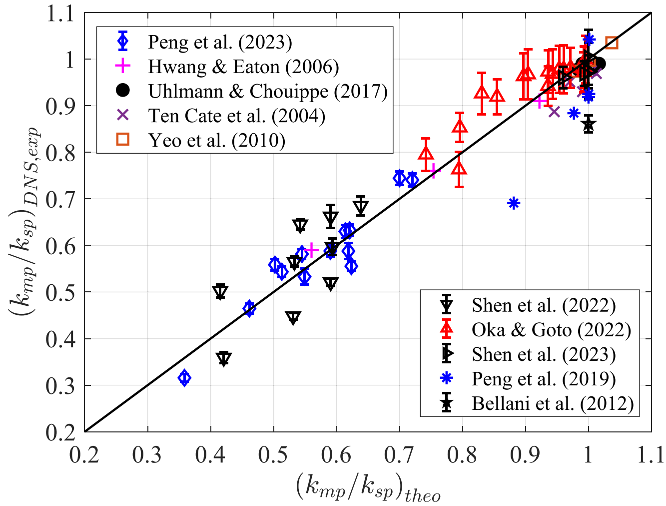

FIG. 1. Comparison of turbulence modulation obtained in simulations/experiments (y axis) against theoretical prediction using Eq. (4) (x axis).

related as given in Eq. (6). Figure 1 includes error bars for those data points whose uncertainties are available. The R^2 value for the curve fit is 0.9269.

As can be seen in Fig. 1, in most prior investigations, when gravitational effect is either absent or weak, turbulence is generally attenuated and the attenuation can be substantial (multiphase turbulence can be as low as 30% of single-phase counterpart). In other words, in the absence of gravitational effect, the effect of suspended particles is mostly dissipative. As will be seen below, with the inclusion of strong particle settling due to gravity, a mechanism of turbulence production is introduced which can contribute to turbulence augmentation.

For heavy particles, the coefficient C' is larger than unity, and in Eq. (7) the difference is expressed as two parts: one that depends on excess mass loading by the particles and the other depends on the particle Stokes number. The first factor is motivated by Peng *et al.* [6], who observed increased mass of the multiphase flow to be an important parameter. The rationale is that with increasing mixture density, the fluid velocity fluctuation decreases. However, with increased mass loading, particles become less responsive, and the fluid velocity fluctuation is less influenced by the particles. Therefore, here we find it is necessary to cap the value of C'. The Stokes number-dependent second factor is motivated by the observation in [5] that when St_k increases above a few hundred, the attenuation effect decreases, partly because for the same volume fraction there are now fewer particles of size substantially larger than the Kolmogorov scale. Furthermore, their motion is largely uncorrelated with the local fluid velocity fluctuations.

Further comparisons are made using the central region of PR turbulent channel flow data. Comparison against ten simulation cases taken from [22,23] are presented in Fig. 1. These ten cases were PR simulations of particle motion within a turbulent channel flow, where there is a nonzero mean streamwise velocity for both the fluid and the particles. Whereas the other cases considered are PR simulations of particle motion in isotropic turbulence without any mean velocity. Since turbulence in a channel is inhomogeneous along the wall-normal direction, here we restrict to fluid and particle statistics gathered in the central region of the channel, away from the bounding walls, where approximate homogeneity is achieved. Note that in a turbulent channel flow, even in the absence of gravitational effect, the average streamwise fluid and particle velocities are different. According to our theoretical formulation, this slip velocity can contribute to increased multiphase turbulence. However, in all ten cases considered, the effect of mean slip velocity is relatively small.

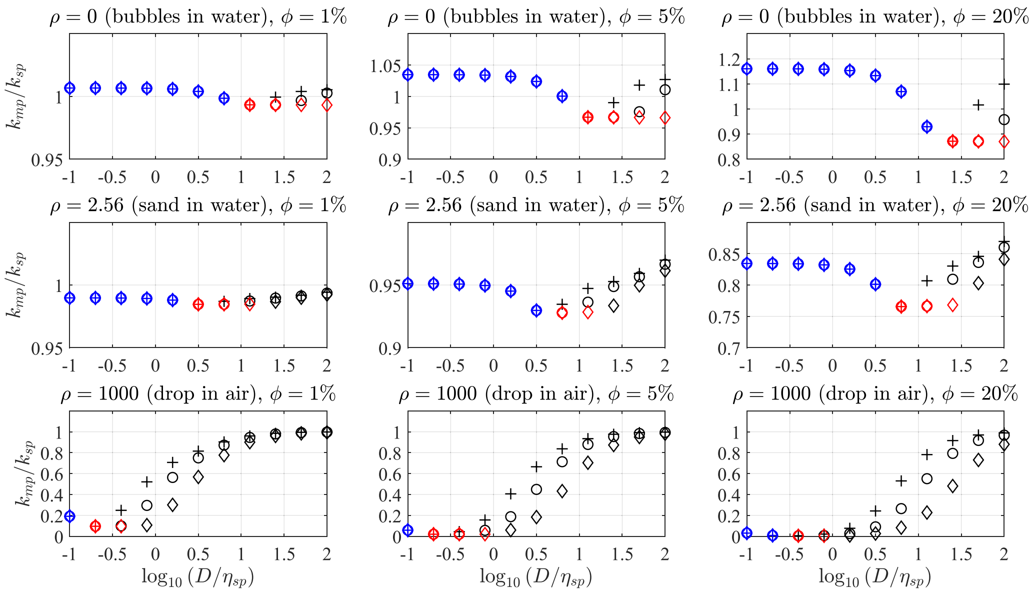

FIG. 2. The ratio of multi to single-phase kinetic energy as a function of D/η for the nonsettling case $u_r = 0$: $Re_\Delta = 5$ (cross), 40 (circle), 400 (diamond). The blue, red, black, and purple color of the symbols indicate the condition falls into regime (i), (ii), (iii), and (iv) of $\Delta u/u_{k,sp}$, respectively.

The results presented are observed to not be sensitive to the precise fit used for C'. An analysis of the prediction presented in Fig. 1 to variations in the model coefficients other than that given in Eq. (7) shows that the overall results are not sensitive. Even a constant value for C' in the range from 1.2 to 1.5 is observed to yield reasonable prediction, although the best fit was with the expression given above. It must be cautioned that the proposed model for C' is adequate for the limited parametric range considered. Better models may be needed with additional data.

IV. PARAMETERIC EFFECT AND COMPARISON

In this section, using the model, we investigate the effects of D/η, Re_Δ, ρ, ϕ, and u_r. The results for $u_r = 0.0$ and 2.0 are presented in Figs. 2 and 3, respectively. The left, middle, and right columns correspond to volume fractions of 1%, 5%, and 20%. The top, middle, and bottom rows correspond to density ratios of zero (bubbles in water), 2.56 (sand particles in water), and 1000 (water droplets in air). The three curves correspond to $Re_\Delta = 5$, 40, and 400 in each plot. In all these calculations we have taken $\epsilon_{mp}/\epsilon_{sp} = 1$. Each symbol is colored according to its slip velocity regime given in Eq. (2). A Matlab code that generated these results is provided as Supplemental Material [35]. This code can be used to calculate turbulence modulation for any given combination of the five parameters.

From Fig. 2, a number of key observations can be made in the limit of zero relative velocity. In the case of small volume fraction of very light particles (bubbles), the turbulence modulation effect is quite small (upper left subplot). However, augmentation and attenuation are observed for particles of size smaller and larger than about $10\eta_{sp}$. This trend of turbulence augmentation at smaller sizes and attenuation at larger sizes is observed more clearly with increasing volume fraction of bubbles. We do not have experimental or PR simulation results that confirm turbulence augmentation of small-sized bubbles. The model prediction of turbulence augmentation can thus be only conjectured mainly due to the reduced effective density of the mixture. For large sized bubbles, as will be shown

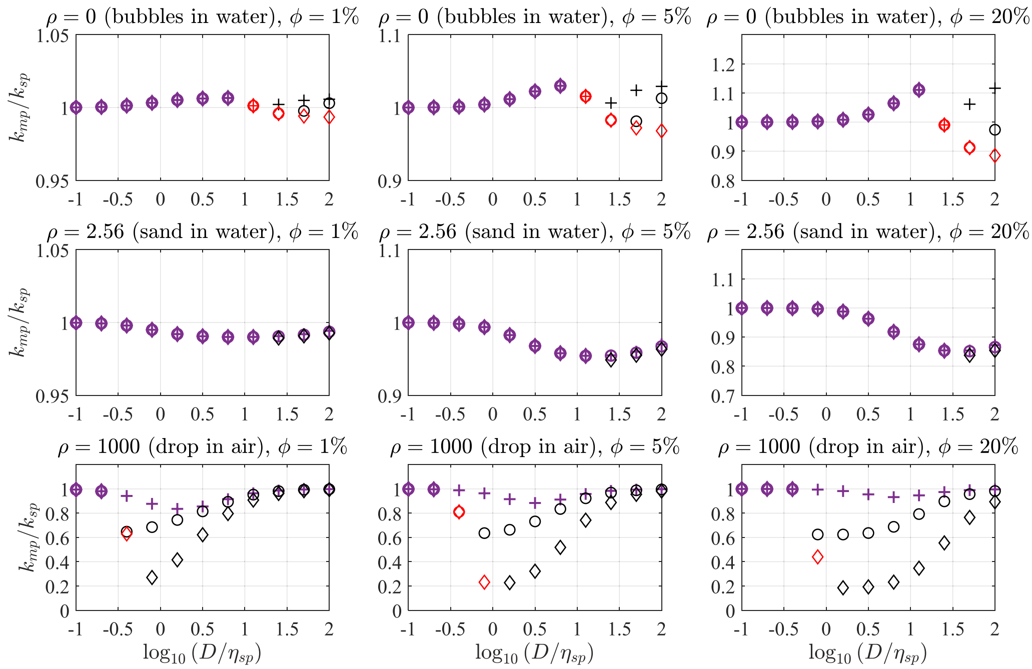

FIG. 3. Same as Fig. 2 but for the settling case $u_r = 2$.

below, the relative velocity increases, and the associated dissipation around the particles contributes to effective turbulence attenuation.

For the density ratio of 2.56 (middle row in Fig. 2), there is no turbulence augmentation, and attenuation is maximized at intermediate particle sizes of $1 < D/\eta_{sp} < 10$. The effect of Re_Δ is not strong. In the case of small particles of $\rho = 1000$, the substantial damping is due to the increase in the mixture density. Small particles tend to move with the fluid and with increased mixture density, for the same energy flux, the intensity of turbulence decreases. In contrast, larger particles remain relatively stationary with their subgrid velocity fluctuations being much smaller than that of the fluid, attenuation is mostly due to dissipation associated with the relative velocity.

In the case of lighter-than-fluid particles (or bubbles), a modest relative velocity of $u_r = 2.0$ does not qualitatively alter turbulence modulation (top row of Fig. 3). Provided the lighter-than-fluid particles are smaller than the Kolmogorov scale, multiphase turbulence is augmented and the increase is substantial with increasing volume fraction. For lighter-than-fluid particles of size larger than the Kolmogorov scale, turbulence is either augmented or attenuated depending on the subgrid Reynolds number. In the case of $\rho = 2.56$, turbulence argumentation is no longer observed. The sub-Kolmogorov scale particles have very small effects on the turbulence. For particles of size larger than the Kolmogorov scale, the magnitude of turbulence damping increases non-monotonically with the particle size, with a peak around $D/\eta \sim 1$ for dilute suspension, which shifts to $D/\eta \approx 1.7$ when the particle volume fraction increases. The magnitude of turbulence damping of heavier than fluid particles of size smaller than the Kolmogorov scale decreases with increasing mean relative velocity, since relative slip contributed to turbulence production. In the limit of very small particles of size $D/\eta \sim 0.1$, turbulence attenuation vanishes. For larger-size heavier-than-fluid particles, the influence of relative velocity is modest at $u_r = 2.0$.

Figures 2 and 3 are composite figures with a lot of information. In these figures, the regime of relative velocity [see Eq. (2)] is also indicated by the color of each symbol: blue indicating small, red indicating medium, and black indicating large inertial particles. The purple color indicates that the

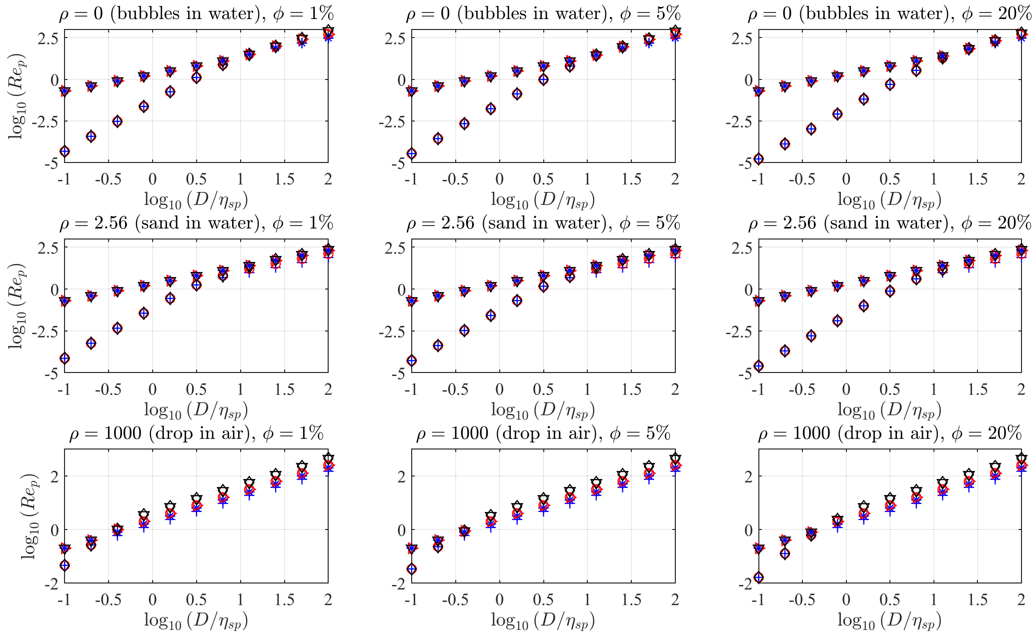

FIG. 4. Particle Reynolds number based on Δu plotted as a function of D/η. The different symbols correspond to $(Re_\Delta, u_r) = (5, 0)$ (blue +), (40,0) (red circle), (400,0) (black diamond), (5,2) (blue asterisk), (40,2) (red right arrowhead), and (400,2) (black downward arrowhead). This figure is for nondimensional mean relative velocity for both $u_r = 0.0$ and $u_r = 2.0$

relative velocity is dictated by mean velocity difference $|\mathbf{u} - \mathbf{v}|$. With increasing u_r, Δu is dictated more by u_r than by cascading turbulence estimated in Eq. (2). For small values of D/η, particles were in regime (i) with $\tau_p/\tau_k < 1$. As shown in Fig. 2 for $u_r = 0.0$, with increasing D/η, the particle Stokes number increased and Δu was given by regime (ii) and then by regime (iii) (i.e., $\tau_p/\tau_k > 1$). This shift from regime (i) to regime (ii) and to regime (iii) occurred for smaller D/η for larger particle-to-fluid ratio. At $u_r = 2.0$ (Fig. 3), Δu is dominated by this mean slip u_r in most cases, except for bubbles of size larger than the Kolmogorov scale, and for larger-size heavier-than-fluid particles at larger subgrid Reynolds numbers. This trend continues for even larger values of u_r.

The large relative velocity contributes to an additional subgrid rate of work and as a result, there is turbulence augmentation in all cases considered. For $u_r = 2$, the augmentation effect reaches a peak at around $D/\eta_{sp} \sim 0.5$ in a dilute system. With increasing volume fraction, the amplitude of peak turbulence augmentation increases and the location shifts to $D/\eta_{sp} \sim 3$. In interpreting the results for large u_r, it must be noted that such large slip velocity either by gravitational settling or inertial response to larger resolved-scale eddies is generally associated with larger values of D/η.

With the relation $\Delta x/\eta = Re_\Delta^{3/4}$, the Gore and Crowe criterion can be rewritten as $D/\eta > 0.1 Re_\Delta^{3/4}$. Nondimensional settling velocity can be expressed as $V_s/u_k = (D/\eta)^2 |\rho - 1|\, g\eta^3/(18\nu^2\,\Phi)$. Now, if we take $\eta \sim 100\,\mu\text{m}$, then for water droplets in air we obtain $V_s/u_k \sim 10(D/\eta)^2$, and for sand particles or bubbles in water we obtain $V_s/u_k \sim (D/\eta)^2$. In general, it can be concluded that larger particle sizes correspond to $u_r \gtrsim 10$. Thus, turbulence enhancement for larger particles is due to production resulting from large settling-induced relative velocity.

Hetsroni [11] suggests that turbulence augmentation for $Re_p > 400$ can now be examined. In Fig. 4 we plot the particle Reynolds number based on relative velocity Δu, for $u_r = 0$ and 2, respectively. In all cases, Re_p approaches a value of $\approx$100 for $D/\eta > 30$, and Re_p increases (decreases) with increasing (decreasing) u_r. For example, at $u_r = 10$, $Re_p \approx 100$ for $D/\eta > 10$. Thus, Hetsroni's criterion for turbulence augmentation can be reinterpreted as a requirement for turbulence production due to large relative velocity. Our results, however, show that turbulence augmentation can occur even in the case of smaller-than-Kolmogorov-scale particles of small relative velocity, provided ρ is not large.

Luo *et al.* [14] predict augmentation when $\rho(D/H)^{-1}Re_b^{-11/16}Re_p > 7000$, while Yu *et al.*'s criterion is $Re_p\phi^{0.1}Re_b^{-0.53}(D/H)^{-0.61}\rho^{-0.065} > 1.55$, where Re_b and H are the bulk Reynolds number and half channel width of the turbulent channel flow, respectively. Again, the significant dependency on Re_p in these criteria can be interpreted as the requirement for sufficient u_r to trigger turbulence enhancement. Both models indicate that turbulence augmentation can happen at smaller Re_p when D and Re_b decrease. However, the current model predicts nonmonotonic dependence of turbulence enhancement on D. Only when the particle size is above a certain threshold would the turbulence enhancement become more significant as particle size reduces. For small particles, turbulence enhancement becomes weaker as the particle size decreases. The dependencies on the density ratio in these two models are different. This difference could indicate the insensitivity of turbulence modulation on the particle density when the work input due to interphase coupling dominates the production of turbulent kinetic energy.

Peng *et al.* [6] only observed turbulence attenuation when finite-size particles with $D/\eta > 1$ and $\rho > 1$ are present, and $u_r = 0$. Hwang and Eaton [19] observed a similar observation in their experiments with smaller particles close to the Kolmogorov length. These results are consistent with the prediction of the present model. In Peng *et al.'s* model, the attenuation becomes more significant when the volume fraction and density ratio increase and the particle size decreases. These trends are also captured well in the present model.

V. CONCLUSIONS

A simple model of turbulence modulation induced by particles/droplets/bubbles is proposed based on an energy flux balance within a representative volume. The size of the representative volume is assumed to fall within the inertial subrange, and be larger than the particle diameter. The energy flux balance considers the work input due to the interphase mean slip and added viscous dissipation occurring at the particle-fluid interfaces due to the relative fluctuating motion. This balance brings in the effects of all important parameters of the system, namely the particle size, volume fraction, density ratio, mean slip velocity, and the representative volume scale Re. This model represents an effort to mechanistically quantify the feedback effects of the dispersed phase on the subgrid Reynolds stress of fluid turbulence in a multiphase large eddy simulation, so a coarse-grained simulation can be reliably conducted.

The model predictions of turbulence modulation agrees well with existing particle-resolved simulations and experimental results. Using this model, we explored the roles of each parameter on turbulence modulation. Both attenuation and augmentation of turbulence are found with light and heavy particles. Turbulence augmentation typically occurs (i) when the system density is reduced by the presence of lighter-than-fluid particles, (ii) when there is significant relative fluctuating motion, and (iii) when relative mean slip between the phases is large. Turbulence damping occurs (i) when the system density is increased by the presence of heavier-than-fluid particles, and (ii) when there is significant dissipative energy loss around the particles. These turbulence augmentation/suppression mechanisms are well studied by previous researchers and the advantage of the present model is its ability to accommodate them. The dependence on particle size is rather complicated and often nonmonotonic. The subgrid Reynolds number in general does not greatly affect the qualitative trends.

We also compare our proposed model to previous models in the literature, in particular concerning the conditions for turbulence augmentation versus attenuation. In general, it is found that the current model can explain the qualitative trends of previous models, and could cover a broader parameter space. With the proposed model, we hope to illustrate not only how the governing parameters affect turbulence modulation, but also point to a physically meaningful way to gather and organize future simulations and experiments on turbulence modulation. As more data becomes available, the model should be refined and extended.

In many practical systems, turbulence modulation by suspended particles, droplets, and bubbles can be far more complicated than the scenario considered in this work. For example, under conditions of substantial heat transfer between the continuous and dispersed phases, buoyancy effects can substantially alter the flow around the particles and thereby the nature of turbulence modulation. Similarly, under conditions of phase change in the form of evaporation, condensation, sublimation, and reverse sublimation, the effect of mass exchange and associated momentum and energy exchanges between the phases can strongly influence turbulence modulation. Investigation of these additional effects must be pursued in the future.

ACKNOWLEDGMENTS

We acknowledge the help of Dr. Jie Shen at SUSTECH for providing us datasets for comparison. LPW has been supported by the National Natural Science Foundation of China (NSFC Awards No. T2250710183, No. U2241269, and No. 11988102).

APPENDIX: COLLISIONAL DISSIPATION MODELING

Inelastic particle collisions contribute to energy dissipation at large particle volume fraction. The dissipation rate within a cell due to particle collisions can be evaluated as the average energy loss per unit collision multiplied by the collision rate. Considering collisions between particles satisfying momentum conservation, the averaged energy loss per collision can be written as

$$\langle \Delta E\rangle = \tfrac{1}{2} C_c\big(1 - e_{\mathrm{wet}}^2\big) m_p \langle \mathbf{v}\rangle^2, \tag{A1}$$

where $\langle \mathbf{v}^2\rangle = \langle \mathbf{v}_1^2\rangle = \langle \mathbf{v}_2^2\rangle$, and angle brackets represent ensemble averaging. The parameter C_c accounts for possible correlation between the precollision velocities of the two colliding particles.

The collision rate per unit volume N_c can be estimated from the collision kernel Γ as [36]

$$N_c = \frac{N^2}{2}\Gamma, \quad \Gamma = 2\pi D^2 \langle |w_r|\rangle\, g_r(D), \tag{A2}$$

where w_r is the radial relative velocity, $g_r(D)$ is the radial distribution function at distance D, and it accounts for the effect of preferential concentration on the collision rate. Substituting $N = 6\phi/(\pi D^3)$ we obtain

$$N_c = \frac{36\phi^2}{\pi D^4}\langle |w_r|\rangle g_r(D). \tag{A3}$$

By combining them, collisional dissipation becomes

$$\epsilon_{\mathrm{coll}} = N_c\langle \Delta E\rangle = 3C_c'\rho\frac{\phi^2}{D}\langle |w_r|\rangle\langle \mathbf{v}\rangle^2, \tag{A4}$$

where $C_c' = C_c(1 - e_{\mathrm{wet}}^2) g_r(D)$.

Using the notation $\langle \mathbf{v}^2\rangle = 2k_p$ and assuming the radial relative velocity to be proportional to Δu, we obtain the last term in the energy balance Eq. (1). All the coefficients in Eq. (A4) have been absorbed into C_{co} in Eq. (1). The ratio between the collision-induced dissipation and the slip velocity-induced dissipation scales as

$$R_c \sim \phi_p\rho\left(\frac{\eta_{k,sp}}{D}\right)^{-1}. \tag{A5}$$

Thus, interparticle collision could significantly contribute to the energy balance for heavy, large-size particles at large volume fractions.

[1] A. Ten Cate, J. J. Derksen, L. M. Portela, and H. E. Van Den Akker, Fully resolved simulations of colliding monodisperse spheres in forced isotropic turbulence, J. Fluid Mech. **519**, 233 (1999).

[2] F. Lucci, A. Ferrante, and S. Elghobashi, Modulation of isotropic turbulence by particles of Taylor length-scale size, J. Fluid Mech. **650**, 5 (2010).

[3] K. Yeo, S. Dong, E. Climent, and M. R. Maxey, Modulation of homogeneous turbulence seeded with finite size bubbles or particles, Int. J. Multiphase Flow **36**, 221 (2010).

[4] H. Gao, H. Li, and L.-P. Wang, Lattice Boltzmann simulation of turbulent flow laden with finite-size particles, Comput. Math. Appl. **65**, 194 (2013).

[5] S. Oka and S. Goto, Attenuation of turbulence in a periodic cube by finite-size spherical solid particles, J. Fluid Mech. **949**, A45 (2022).

[6] C. Peng, Q. Sun, and L.-P. Wang, Parameterization of turbulence modulation by finite-size solid particles in forced homogeneous isotropic turbulence, J. Fluid Mech. **963**, A6 (2023).

[7] M. I. Cantero, S. Balachandar, A. Cantelli, C. Pirmez, and G. Parker, Turbidity current with a roof: Direct numerical simulation of self-stratified turbulent channel flow driven by suspended sediment, J. Geophys. Res.: Oceans **114**, C03008 (2009).

[8] M. Shringarpure, M. I. Cantero, and S. Balachandar, Dynamics of complete turbulence suppression in turbidity currents driven by monodisperse suspensions of sediment, J. Fluid Mech. **712**, 384 (2012).

[9] R. Gore and C. T. Crowe, Effect of particle size on modulating turbulent intensity, Int. J. Multiphase Flow **15**, 279 (1989).

[10] S. Elghobashi and G. Truesdell, On the two-way interaction between homogeneous turbulence and dispersed solid particles. i: Turbulence modification, Phys. Fluids **5**, 1790 (1993).

[11] G. Hetsroni, Particles-turbulence interaction, Int. J. Multiphase Flow **15**, 735 (1989).

[12] P. Bagchi and S. Balachandar, Response of the wake of an isolated particle to an isotropic turbulent flow, J. Fluid Mech. **518**, 95 (2004).

[13] T. Tanaka and J. K. Eaton, Classification of turbulence modification by dispersed spheres using a novel dimensionless number, Phys. Rev. Lett. **101**, 114502 (2008).

[14] K. Luo, M. Luo, and J. Fan, On turbulence modulation by finite-size particles in dilute gas-solid internal flows, Powder Technol. **301**, 1259 (2016).

[15] M. I. Cantero, S. Balachandar, and G. Parker, Direct numerical simulation of stratification effects in a sediment-laden turbulent channel flow, J. Turbul. **10**, N27 (2009).

[16] J. S. Salinas, S. Balachandar, M. Shringarpure, J. Fedele, D. Hoyal, S. Zuñiga, and M. I. Cantero, Anatomy of subcritical submarine flows with a lutocline and an intermediate destruction layer, Nat. Commun. **12**, 1649 (2021).

[17] A. Chouippe and M. Uhlmann, On the influence of forced homogeneous-isotropic turbulence on the settling and clustering of finite-size particles, Acta Mech. **230**, 387 (2019).

[18] J. Shen, C. Peng, J. Wu, K. L. Chong, Z. Lu, and L.-P. Wang, Turbulence modulation by finite-size particles of different diameters and particle–fluid density ratios in homogeneous isotropic turbulence, J. Turbul. **23**, 433 (2022).

[19] W. Hwang and J. K. Eaton, Homogeneous and isotropic turbulence modulation by small heavy ($St \sim 50$) particles, J. Fluid Mech. **564**, 361 (2006).

[20] W. Hwang and J. K. Eaton, Turbulence attenuation by small particles in the absence of gravity, Int. J. Multiphase Flow **32**, 1386 (2006).

[21] G. Bellani, M. L. Byron, A. G. Collignon, C. R. Meyer, and E. A. Variano, Shape effects on turbulent modulation by large nearly neutrally buoyant particles, J. Fluid Mech. **712**, 41 (2012).

[22] C. Peng, O. M. Ayala, and L.-P. Wang, A direct numerical investigation of two-way interactions in a particle-laden turbulent channel flow, J. Fluid Mech. **875**, 1096 (2019).

[23] J. Shen, C. Peng, Z. Lu, and L.-P. Wang, Turbulence modulation by finite-size particles of different diameters and particle–fluid density ratios in a channel, Inter. J. Multiphase flow **170**, 104659 (2024).

[24] S. Balachandar, *Fundamentals of dispersed multiphase flows* (Cambridge University Press, Cambridge, UK, 2024).

[25] A. Chouippe and M. Uhlmann, Forcing homogeneous turbulence in direct numerical simulation of particulate flow with interface resolution and gravity, Phys. Fluids **27**, 123301 (2015).

[26] J. Richardson and W. Zaki, The sedimentation of a suspension of uniform spheres under conditions of viscous flow, Chem. Eng. Sci. **3**, 65 (1954).

[27] D. Gidaspow, *Multiphase flow and fluidization: continuum and kinetic theory descriptions* (Academic press, 1994).

[28] S. Tenneti, R. Garg, and S. Subramaniam, Drag law for monodisperse gas–solid systems using particle-resolved direct numerical simulation of flow past fixed assemblies of spheres, Int. J. Multiphase Flow **37**, 1072 (2011).

[29] S. Elghobashi, On predicting particle-laden turbulent flows, Appl. Sci. Res. **52**, 309 (1994).

[30] S. Balachandar and J. K. Eaton, Turbulent dispersed multiphase flow, Annu. Rev. Fluid Mech. **42**, 111 (2010).

[31] S. Balachandar, A scaling analysis for point–particle approaches to turbulent multiphase flows, Int. J. Multiphase Flow **35**, 801 (2009).

[32] Y. Ling, M. Parmar, and S. Balachandar, A scaling analysis of added-mass and history forces and their coupling in dispersed multiphase flows, Int. J. Multiphase Flow **57**, 102 (2013).

[33] C. Tchen, *Mean value and correlation problems connected with the motion of small particles in a turbulent fluid* (Springer, Dordrecht, 1947).

[34] L.-P. Wang and D. E. Stock, Dispersion of heavy particles by turbulent motion, J. Atmos. Sci. **50**, 1897 (1993).

[35] https://github.com/jasonshen1990/Physics-based-multiphase-subgridmodeling.

[36] L.-P. Wang, A. S. Wexler, and Y. Zhou, Statistical mechanical description and modelling of turbulent collision of inertial particles, J. Fluid Mech. **415**, 117 (2000).